A Journal of the Gesellschaft Deutscher Chemiker

Angewandte International Edition

GDCh

Chemie

www.angewandte.org

Accepted Article

Title: Enhancing hydrogen evolution activity of Au(111) in alkaline media through molecular engineering of a 2D polymer

Authors: Patrick Alexa, Juan Manuel Lombardi, Paula Abufager, Heriberto Fabio Busnengo, Doris Grumelli, Vijay S. Vyas, Frederik Haase, Bettina V. Lotsch, Rico Gutzler, and Klaus Kern

To be cited as: *Angew. Chem. Int. Ed.* 10.1002/anie.201915855
Angew. Chem. 10.1002/ange.201915855

Link to VoR: http://dx.doi.org/10.1002/anie.201915855
http://dx.doi.org/10.1002/ange.201915855

WILEY-VCH

10.1002/anie.201915855

Enhancing hydrogen evolution activity of Au(111) in alkaline media through molecular engineering of a 2D polymer

Patrick Alexa,[a] Juan Manuel Lombardi,[b] Paula Abufager,[b] Heriberto Fabio Busnengo,[b] Doris Grumelli,[c] Vijay S. Vyas,[a,†] Frederik Haase,[a,‡] Bettina V. Lotsch,[a,d] Rico Gutzler,*[a] Klaus Kern[a,e]

[a] Max Planck Institute for Solid State Research, Heisenbergstrasse 1, 70569 Stuttgart, Germany
E-mail: r.gutzler@fkf.mpg.de

[b] Instituto de Física Rosario and Universidad Nacional de Rosario, CONICET-UNR, S2000EZO Rosario, Argentina

[c] Instituto de Investigaciones Fisicoquímicas Teóricas y Aplicadas (INIFTA), Facultad de Ciencias Exactas, Universidad Nacional de La Plata, CONICET, 1900, La Plata, Argentina

[d] Department of Chemistry, University of Munich (LMU), Butenandtstraße 5-13, 81377 München, Germany

[e] Institut de Physique, École Polytechnique Fédérale de Lausanne (EPFL), 1015 Lausanne, Switzerland

[†] present address: Department of Chemistry, Marquette University, Milwaukee WI - 53233

[‡] present address: Institute for Integrated Cell-Material Sciences (WPI-iCeMS), Kyoto University, iCeMS Research Bldg, Yoshida, Sakyo-ku, Kyoto 606-8501, Japan

Abstract

The electrochemical splitting of water holds promise for the storage of energy intermittently produced by renewable energy sources. The evolution of hydrogen currently relies on the use of platinum as a catalyst – which is scarce and expensive – and ongoing research is focused towards finding cheaper alternatives. In this context, 2D polymers grown as single layers on surfaces have emerged as porous materials with tunable chemical and electronic structure and can be used for improving catalytic activity of metal surfaces. Here, we use designed organic molecules to fabricate covalent 2D architectures by an Ullmann type coupling reaction on Au(111). The polymer patterned gold electrode exhibits up to three times higher hydrogen evolution reaction activity compared to bare gold. Through rational design of the polymer on the molecular level we can engineer hydrogen evolution activity in an approach that is easily extendible to other electrocatalytic reactions.

10.1002/anie.201915855

Water electrolyzers, in which H_2O is split into molecular hydrogen and oxygen, are suitable devices for the storage of intermittently generated excess energy from renewable energy sources like sun and wind power.[1,2] This power-to-fuel approach converts electricity into chemical energy and generates an energy-dense fuel (H_2) that can readily be stored and transported. On the route towards cheap and efficient electrocatalytic water splitting catalysts, the replacement of platinum group metals as catalysts for the hydrogen evolution (HER) half-cell reaction is a primary milestone.[3] Whereas platinum and platinum group metals function best under acidic conditions at low pH values,[4] these strongly corrosive conditions inhibit the use of cheaper transition metal based catalysts, and highly acidic proton exchange membrane systems are costly and suffer from concerns regarding their stability. More challenging, however, is the lower activity of hydrogen evolution catalysts in alkaline media compared to acidic media.[5] For equal overpotentials, exchange current densities are commonly smaller in alkaline electrolyte compared to acidic electrolyte, and current efforts are underway to close this gap.[6–8] The rate limiting step here seems to be the scission of the HO–H bond in the Volmer step, which precedes the adsorption of hydrogen, and which can be accelerated by designing adequate co-catalysts. One approach is the deposition of a material that stabilizes H_2O close to the electrode via hydrogen bonding.[6,9] The increased interaction results in faster generation of adsorbed hydrogen, which can then combine to form H_2 on platinum, effectively leading to higher HER activity.

Elaborating on this concept, we use molecular engineering to pattern a well-defined gold electrode surface with an organic polymer of tunable chemical structure with the aim of increasing HER activity at pH 13. The 2D porous single-layer polymer is structurally similar to the organic sheets that build up 2D covalent organic frameworks (COFs). COFs have recently emerged as active photocatalysts for hydrogen production,[10–12] in which the organic framework can efficiently absorb light due to their suitable band gap. On single-crystal electrode supports, related single-layer 2D polymers can be fabricated that pattern the electrode surface with a covalent porous network.[13–15] Through a deliberate choice of the chemical structure of the polymer, we can pattern the gold electrode on the nanoscale with hydrogen bonding sites. In this organic-inorganic hybrid catalyst, the polymer functions as a co-catalyst that alters the binding strength of the reactants at the gold surface, which ultimately increases HER activity.

In this comprehensive study, we use scanning tunelling microscopy (STM), X-ray photoelectron spectroscopy (XPS), electrochemical (EC) measurements, and density functional theory (DFT) calculations to draw a concice picture of the catalyst before and after HER. Three different brominated precursor molecules with varying nitrogen content were used for on-surface polymer synthesis (Fig. 1a) (1,3,5-tris-(4-bromophenyl)-benzene (**N_0**), 2,4,6-tris-(4-bromophenyl)-1,3,5-triazine (**N_3**), and 2,2',2''-(benzene-1,3,5-triyl)-tris-(5-bromopyrimidine) (**N_6**)). Established Ullmann-type coupling procedures[16–19] on an atomically clean Au(111) substrate allow patterning the surface with a one-monolayer thin porous 2D network (Fig. 1b). For the three precursor molecules **N_0**, **N_3**, and **N_6**, the corresponding covalent 2D polymers **P-N_0**, **P-N_3**, and **P-N_6** exhibit an amorphous network structure with pores of different shapes, mostly hexagons, pentagons, and heptagons. The repeat unit of the polymer consists of two debrominated precursor molecules. **P-N_0** is composed purely of carbon and hydrogen, whereas **P-N_3** contains triazine heterocycles at the vertices of the network and **P-N_6** contains pyrimidine groups in the network's 'struts' (cf. Fig. 1a). All three polymers are physisorbed on the Au(111) surface. The void pores

10.1002/anie.201915855

expose the underlying bare substrate and leave it accessible to electrolyte molecules. The polymer-covered gold substrates were tested for their properties as electrocatalysts, in particular for HER.

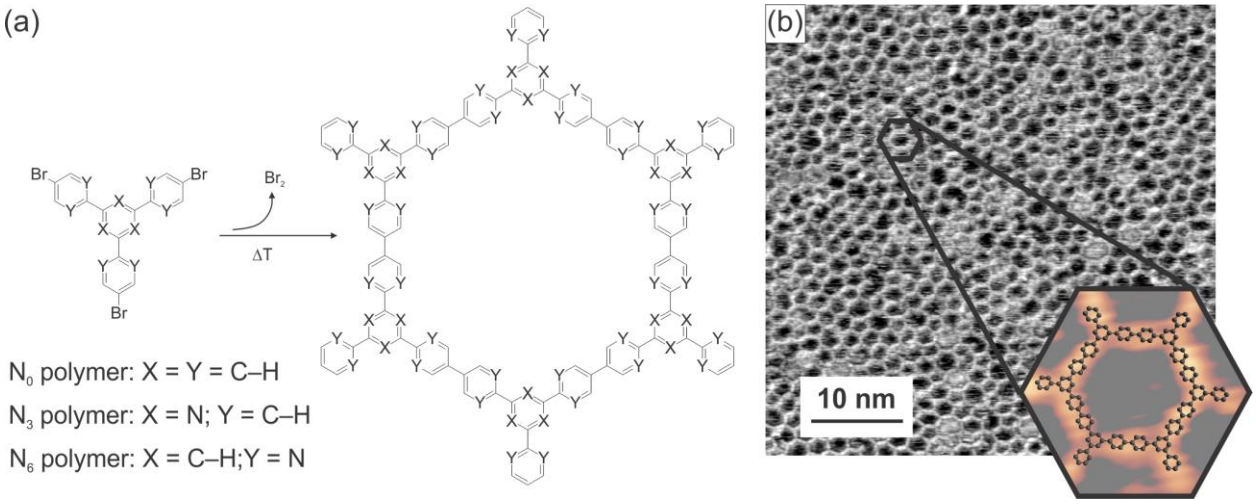

Figure 1: Tunable 2D polymers for electrocatalytic hydrogen evolution: (a) Synthesis scheme of polymerization synthesis. (b) STM topograph (*I* = 175pA, *U* = −1.2 V) of **P-N$_0$**, low right corner shows an enlargement of a hexagonal pore with a molecular model overlaid.

The polymers on the Au(111) surface show characteristic EC signals in cyclic voltammograms (Fig. 2a, **P-N$_0$** (turquoise), **P-N$_3$** (blue) and the **P-N$_6$** (purple)) in the potential window –0.70 to –0.95 $V_{Ag/AgCl}$ which are not present on the bare Au(111) surface (see supporting Information for further discussion). The presence of these signals is an electrochemical indicator for the polymers and goes along with an increased HER activity. Polarization curves at more negative potentials of bare Au(111), **P-N$_0$**, **P-N$_3$** and **P-N$_6$** are shown in Fig. 2b and exhibit different current densities for negative potentials as a consequence of different HER activities. Current densities are depicted with respect to the geometrical area of the crystal; electrochemically active surface areas are equal for all considered systems (see Fig. S3 supporting information). Bare Au(111) shows a current density of −0.16 mA cm^{-2} at a potential of −1.3 $V_{Ag/AgCl}$, while the presence of the **P-N$_3$** increases this value more than three-fold to −0.55 mA cm^{-2}. **P-N$_0$** and **P-N$_6$** reach both a current density of −0.27 mA cm^{-2}, almost twice as large as Au(111). For comparison, the overpotentials vs. the reversible hydrogen electrode at –0.2 mA cm^{-2} are –0.23 V (**P-N$_3$**), –0.29 V (**P-N$_0$**), –0.30 V (**P-N$_6$**), and –0.35 V (gold).

10.1002/anie.201915855

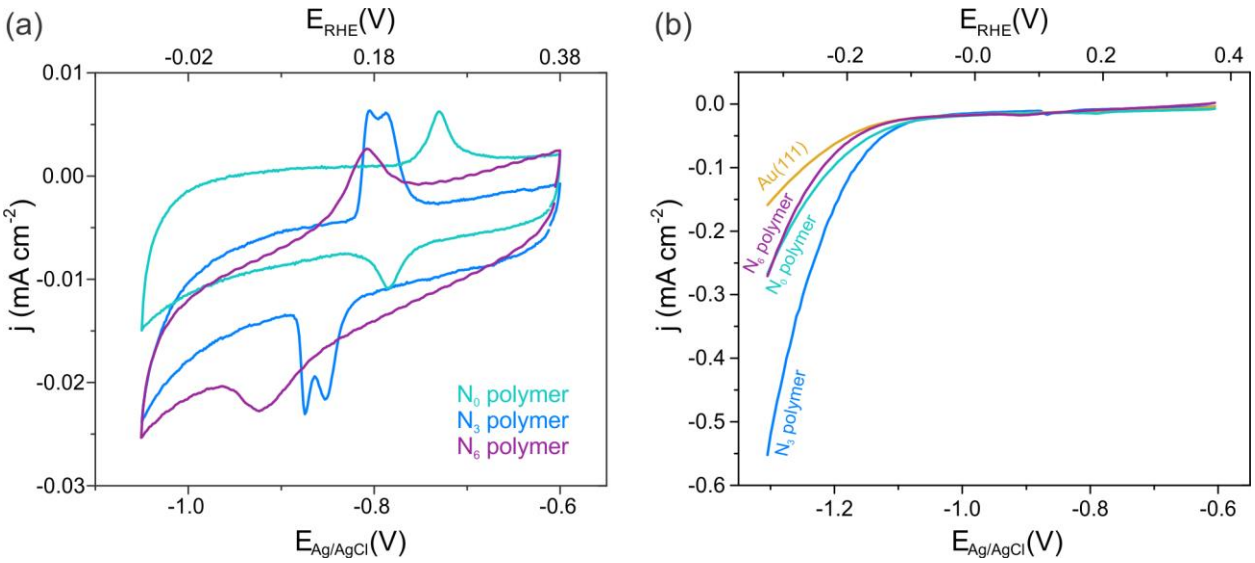

Figure 2: (a) Cyclic voltammograms in 0.1 M Ar saturated NaOH solution for **P-N$_0$** polymer (turquoise), **P-N$_3$** (blue) and **P-N$_6$** (purple). (b) Polarization curves at 0.05 V s^{-1} in 0.1 M Ar saturated NaOH solution for bare Au(111) (yellow), **P-N$_0$** polymer (turquoise), **P-N$_3$** (blue) and **P-N$_6$** (purple).

To ensure that the polymer is present during catalysis and does not decompose prior or during HER, we performed X-ray photoelectron spectroscopy (XPS) before and after catalysis of all three polymers. Exemplarily, Fig. 3 shows the characterization of **P-N$_3$** together with typical STM data acquired before and after HER (three polarization scans up to −1.2 $V_{Ag/AgCl}$), the spectra and images for **P-N$_0$** and **P-N$_6$** are shown in the supporting information. No changes are apparent in STM, apart from the filling of the pores with what presumably are residues of the electrolyte (Fig. 3 a,b), which is also reflected in the unaltered C 1s core level signal (Fig. 3d). The signal around 284 eV is due to the carbon in the phenyl rings in the polymer, the smaller signal around 286 eV originates from the carbon atoms in the triazine ring. In the N 1s spectrum before HER, only one component of the triazine nitrogen atoms is observable (Fig. 3c). After HER, however, additional signals are observed at higher binding energy around 400 eV and 401 eV. These additional signals potentially come from the interaction of the nitrogen atoms with other species like hydrogen. Literature confirms that attaching hydrogen to nitrogen is shifting the core level to higher binding energy, for example for protonated amino groups[20], where the signal is shifted from ~399.3 eV to ~401.2 eV, or in free-base porphyrins[21], where the iminic nitrogen is observed at 398.0 eV and pyrrolic nitrogen at 400.1 eV. The hydrogen species attached to the polymer at its nitrogen sites is an intermediate of HER and its implications for the reaction mechanism will be discussed below. It is noteworthy that exposure of **P-N$_3$** to the electrolyte without applying any potential already leads to the appearance of a peak at 400 eV, indicative of the interaction of water with the polymer (see Fig. S8 supporting information). From this observation we can infer that the nitrogen in the polymer acts as interaction site for water molecules, which stabilizes H_2O close to the gold electrode. HER activity starts to decrease after extended catalytic turnover (Fig. S5 supporting information), possibly due to degradation of the polymer (see XPS in Fig. S7).

10.1002/anie.201915855

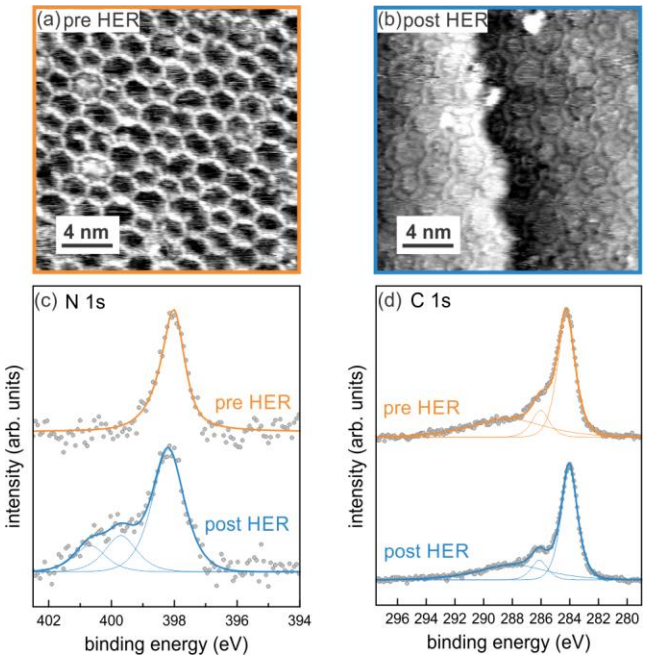

Figure 3: **P-N_3** characterization before and after HER: (a) STM image before the electrochemical experiment, and (b) recorded after the electrochemical experiment. (c) XPS spectra of the N 1s core level, orange: before HER, blue: after HER, (d) XPS spectra of the C 1s core level, orange: before HER, blue: after HER.

Understanding the observed trend in HER activity (**P-N_3** > **P-N_6** ≈ **P-N_0** > Au(111)) calls for the help of theoretical support that can deliver insight into the different steps of H_2O conversion into hydrogen molecules. Catalytic activity is usually rationalized in terms of the Sabatier principle, which describes the optimum catalyst such that the interaction of adsorbed intermediate species is neither too weak nor too strong. If the interaction is too weak, the intermediate does not bind to the catalyst, but if it is too strong, it is too stable and the reaction cannot proceed. The Sabatier principle is graphically illustrated by plotting an observable parameter connected with the catalyst activity (e.g. the electrochemical current in electrocatalysis) as a function of one or more adequate properties quantifying the strength of the interaction of the reaction intermediates with the catalyst (e.g. heats of adsorption). This gives rise to the so-called volcano plots, with the largest catalytic activity (i.e. the summit of the volcano) being obtained for the catalyst characterized by the "just right" value of the reaction descriptor(s).

The usual descriptor used for the HER is the hydrogen binding energy (HBE).[22–24] However, since the HBE is an intrinsic property of the catalyst, it is not suitable to account for the effect of external parameters like the pH of aqueous electrolytes. Since the electrode surface in an aqueous electrolyte is covered with water, it is likely that the adsorption/desorption of hydrogen is accompanied by desorption/readsorption of water.[25,26] Thus, a more suitable descriptor proposed recently is the apparent hydrogen binding energy (HBE_{app}), which also takes the water binding energy (WBE) into account, HBE_{app}=HBE−WBE.[25] The HBE_{app} descriptor includes pH-dependency in describing electrocatalytic activities, whereby H adsorption remains as a microscopic reaction step for both acid

and base electrolytes. Since it was recently shown that the adsorption of hydrogen is the critical reaction step for all pH values,[27] we rationalize in the following our observed HER activities using the modified H-binding energy HBE_{app} as a descriptor.

As Pt(111) is the benchmark catalyst for HER, it is expected that the most active catalyst of the investigated systems has an HBE_{app} value close to Pt(111). We used DFT to compute HBE, WBE, and HBE_{app} for **P-N$_3$**, **P-N$_0$**, **P-N$_6$**, and Au(111) as well as for Pt(111). This requires searching for the optimum adsorption geometry of H and H_2O on all the investigated systems. We found the optimum adsorption geometry for H_2O on all investigated polymers at the vertices of the organic network where water molecules form hydrogen bonds with the polymers involving the N atoms for **P-N$_3$** and **P-N$_6$** (see supporting information Figs. S9).

For atomic hydrogen on **P-N$_3$** and **P-N$_6$**, the most favorable adsorption site is at the nitrogen atoms, in line with the N 1s XPS data shown above. These results point to N atoms acting as docking sites for both H_2O and H. In contrast, the optimal adsorption environment of H on **P-N$_0$** is the same as on bare Au(111). H prefers the adsorption site on threefold-hollow sites of Au(111) rather than in proximity to the polymer (Supporting Information, Fig. S10), which is also in line with the unaltered C 1s XPS signal.

Figure 4a shows the values of WBE and HBE_{app} corresponding to the optimum adsorption geometries found for the three polymer-decorated surfaces and for Au(111). The HBE_{app} (WBE) values obtained for **P-N$_3$**, **P-N$_6$**, **P-N$_0$**, and Au(111) are +0.02 eV (−0.38 eV), +0.32 eV (−0.77 eV), +0.64 eV (−0.44 eV), and +0.51 eV (−0.31 eV) respectively. The HBE_{app} in Fig. 4a is the energy difference between the energies represented in the right gray panel (H adsorption) and in the central panel (H_2O adsorption). In light of the previous discussion, the activity of each catalyst correlates with its HBE_{app} value and can be compared to the one of Pt(111), which is $HBE_{app,Pt}$=−0.07 eV. The measured values of the current densities (j) as a function of the computed values of HBE_{app} are shown in Fig. 4b. The value of $HBE_{app,Pt}$ is indicated with a vertical dashed line. According to the previous analysis, the polymer with the HBE_{app} value closest to Pt is **P-N$_3$**, which is the one with the largest HER activity. We connect the high activity of **P-N$_3$** to an optimized balance between water and hydrogen binding energies that are similar to Pt(111). Compared with **P-N$_3$**, **P-N$_6$** binds H_2O stronger than H, which diminishes electrocatalytic activity, in good agreement with experiments. Hydrogen adsorption on Au(111) becomes endothermic when considering WBE, inducing a further increase of HBE_{app} and a reduction of its expected catalytic activity with respect to **P-N$_3$** and **P-N$_6$**. Thus, our theoretical results are in line with the experimental trend of HER activities: **P-N$_3$** > **P-N$_6$** > Au(111), although there remains a discrepancy concerning the **P-N$_0$** system. The HBE_{app} descriptor does not account for the measured activity of **P-N$_0$**, which is higher than the activity of Au(111) and similar to the one obtained for **P-N$_6$**. This result indicates that other reaction steps might be rate delimiting and further parameters are required for a full description of all the investigated systems.

For instance, the activity of the supported **P-N$_0$** and **P-N$_3$** polymers might be reinforced due to the particular binding geometry. Our calculations show that single H_2O molecules adsorb parallel to the surface on top sites, which is in good agreement with previous theoretical results.[28] In the case of **P-N$_0$** and **P-N$_3$** one hydrogen atom of the water molecule points downwards towards the gold electrode (H-down configuration) while for **P-N$_6$**, H_2O lies parallel to the surface forming H-bonds with two N atoms of

10.1002/anie.201915855

the polymer. The H-down geometry of H_2O (Fig. 4a) favors interaction with the gold electronic states, and consequently electrons transfer into the antibonding $4a_1$ and $2b_2$ orbitals of water (Fig. 4c). As a consequence, this might destabilize the H−O bond, increasing water dissociation and generation of H. Similar overlap of the unoccupied antibonding orbitals of water is absent on Au(111) and **P-N$_6$**. We note that a similar H-down configuration that we propose to facilitate reductive charge transfer into H_2O is observed in calculations for bare Au(111) and Pt(111).[29] At room temperature, the water layer on gold becomes disordered whereas on platinum it remains at least partially in the H-down configuration; should this adsorption geometry be responsible for the high activity of Pt, then we can expect **P-N$_0$** and also **P-N$_3$** to work along the same way. Acknowledging that hydrogen adsorption is the relevant descriptor for HER activity, we can thus correlate catalytic activity to the binding energies of H_2O and H on the polymer-decorated surface. Further properties might also influence the details of the reaction but are probably not the rate-limiting steps; for example, once H_2 is formed at a vertex of the polymer, H_2 abstraction is accompanied by a barrier not larger than ~0.17 eV, which is certainly much lower than all other barriers.

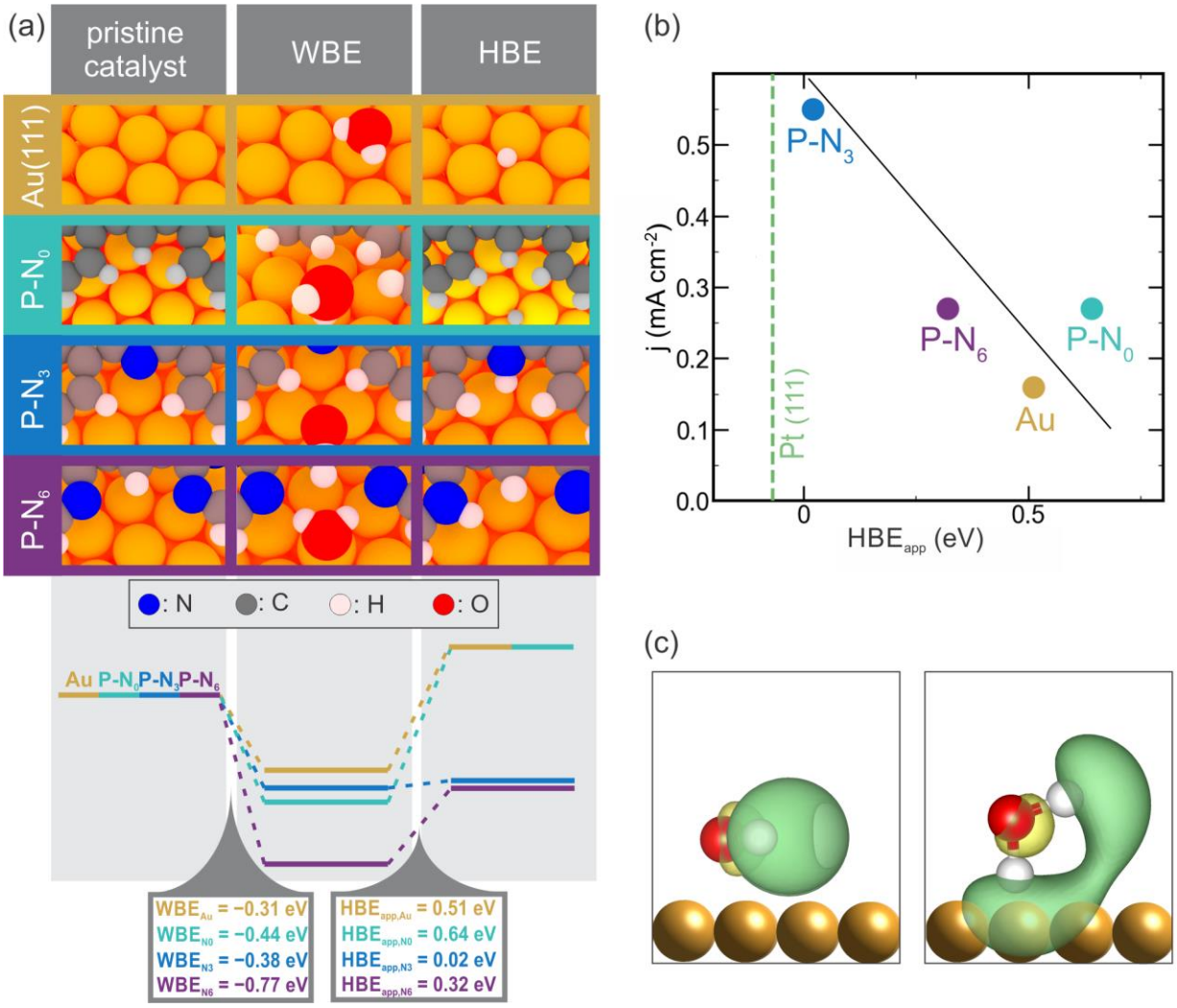

Figure 4: (a) Energy diagram for H_2O and H adsorption and adsorption geometries on Au(111) and at the polymers. (b) Plot of HER activity vs. calculated HBE_{app}, the linear line is to guide the eye. (c) Antibonding orbitals of water for parallel and H-down adsorption configurations.

In conclusion, hydrogen evolution activity of a gold electrode in alkaline electrolyte is enhanced through patterning the electrode surface with a porous two-dimensional polymer. The polymer provides docking sites for H_2O and H through hydrogen bonds and increases the binding energy and residence time close to the electrode, which consequently increases catalytic activity. Systematic engineering the hydrogen bonding sites of the polymer is used to adjust HER activity. Our results highlight the advantage of controlling reactant interaction with the electrode patterned with porous polymers to achieve hybrid organic/inorganic catalysts: The interaction of reactants and intermediate products with the electrode is fine-tuned by providing adequate docking sites. The binding energy can be dialed-in such that the optimal energy on the abscissa of the corresponding volcano plot can be achieved for any given metal catalyst just by encoding suitable interaction sites into the precursor molecules. One can envision that different docking sites such as hydroxyl groups or sulfur hetero atoms on the polymer further tweak hydrogen bonding interactions and position the reactants in a suitable geometry for increased activity. This paves the way for enhancing catalytic activity not only of HER but also for other electrocatalytic reactions on earth-abundant transition metal catalysts.

Acknowledgements

Financial support by the ERC Starting Grant (project COF Leaf, grant number 639233), the DFG cluster of excellence “e-conversion” and the Center for NanoScience (CeNS) is gratefully acknowledged by B.V.L . J. M. L, P. A. and H. F. B acknowledge financial support from ANPCyT PICT-2750 and the computational time provided by the CCT-Rosario computational center and Computational Simulation Center (CSC) for Technological Applications, members of the High Performance Computing National System (SNCAD-MincyT Argentina)

Keywords: hydrogen evolution reaction • hybrid catalyst • STM • XPS • DFT

Bibliography

[1] F. M. Mulder, *J. Renew. Sustain. Energy* **2014**, *6*, 033105.

[2] J. H. Montoya, L. C. Seitz, P. Chakthranont, A. Vojvodic, T. F. Jaramillo, J. K. Nørskov, *Nat. Mater.* **2016**, *16*, 70–81.

[3] Z. W. Seh, J. Kibsgaard, C. F. Dickens, I. Chorkendorff, J. K. Nørskov, T. F. Jaramillo, *Science* **2017**, *355*, eaad4998.

[4] N. Mahmood, Y. Yao, J.-W. Zhang, L. Pan, X. Zhang, J.-J. Zou, *Adv. Sci.* **2018**, *5*, 1700464.

[5] W. Sheng, H. A. Gasteiger, Y. Shao-Horn, *J. Electrochem. Soc.* **2010**, *157*, B1529.

[6] R. Subbaraman, D. Tripkovic, D. Strmcnik, K.-C. Chang, M. Uchimura, A. P. Paulikas, V. Stamenkovic, N. M. Markovic, *Science* **2011**, *334*, 1256–1260.

[7] R. Subbaraman, D. Tripkovic, K.-C. Chang, D. Strmcnik, A. P. Paulikas, P. Hirunsit, M. Chan, J. Greeley, V. Stamenkovic, N. M. Markovic, *Nat. Mater.* **2012**, *11*, 550–557.

[8] H. Vrubel, X. Hu, *Angew. Chemie* **2012**, *124*, 12875–12878.

[9] X. Yu, J. Zhao, L.-R. Zheng, Y. Tong, M. Zhang, G. Xu, C. Li, J. Ma, G. Shi, *ACS Energy Lett.* **2018**, *3*, 237–244.

[10] L. Stegbauer, K. Schwinghammer, B. V. Lotsch, *Chem. Sci.* **2014**, *5*, 2789–2793.

[11] V. S. Vyas, F. Haase, L. Stegbauer, G. Savasci, F. Podjaski, C. Ochsenfeld, B. V. Lotsch, *Nat. Commun.* **2015**, *6*, 8508.

[12] T. Banerjee, K. Gottschling, G. Savasci, C. Ochsenfeld, B. V. Lotsch, *ACS Energy Lett.* **2018**, *3*, 400–409.

[13] L. Grill, S. Hecht, *Nat. Chem.* **2020**, *12*, 115–130.

[14] J. W. Colson, W. R. Dichtel, *Nat. Chem.* **2013**, *5*, 453–465.

[15] Q. Shen, H.-Y. Gao, H. Fuchs, *Nano Today* **2017**, *13*, 77–96.

[16] W. Wang, X. Shi, S. Wang, M. A. Van Hove, N. Lin, *J. Am. Chem. Soc.* **2011**, *133*, 13264–13267.

[17] Q. Fan, J. M. Gottfried, J. Zhu, *Acc. Chem. Res.* **2015**, *48*, 2484–2494.

[18] J. Eichhorn, D. Nieckarz, O. Ochs, D. Samanta, M. Schmittel, P. J. Szabelski, M. Lackinger, *ACS Nano* **2014**, *8*, 7880–7889.

[19] S. Clair, D. G. de Oteyza, Chem. Rev. **2019**, *119*, 4717–4776

[20] N. Graf, E. Yegen, T. Gross, A. Lippitz, W. Weigel, S. Krakert, A. Terfort, W. E. S. Unger, *Surf. Sci.* **2009**, *603*, 2849–2860.

[21] M. Chen, X. Feng, L. Zhang, H. Ju, Q. Xu, J. Zhu, J. M. Gottfried, K. Ibrahim, H. Qian, J. Wang, *J. Phys. Chem. C* **2010**, *114*, 9908–9916.

[22] S. Trasatti, *J. Electroanal. Chem. Interfacial Electrochem.* **1972**, *39*, 163–184.

[23] J. K. Nørskov, T. Bligaard, A. Logadottir, J. R. Kitchin, J. G. Chen, S. Pandelov, U. Stimming, *J. Electrochem. Soc.* **2005**, *152*, J23–J26.

[24] W. Sheng, M. Myint, J. G. Chen, Y. Yan, *Energy Environ. Sci.* **2013**, *6*, 1509–1512.

[25] J. Zheng, J. Nash, B. Xu, Y. Yan, *J. Electrochem. Soc.* **2018**, *165*, H27–H29.

[26] T. Cheng, L. Wang, B. V. Merinov, W. A. Goddard, *J. Am. Chem. Soc.* **2018**, *140*, 7787–7790.

[27] J. Durst, A. Siebel, C. Simon, F. Hasché, J. Herranz, H. A. Gasteiger, *Energy Environ. Sci.* **2014**, *7*, 2255–2260.

[28] P. Tereshchuk, J. L. F. Da Silva, *J. Phys. Chem. C* **2012**, *116*, 24695–24705.

[29] S. Schnur, A. Groß, *New J. Phys.* **2009**, *11*, 125003.